Cell Metabolism
Article

Protection from Obesity and Diabetes by Blockade of TGF-β/Smad3 Signaling

Hariom Yadav,[1] Celia Quijano,[2,10] Anil K. Kamaraju,[1] Oksana Gavrilova,[3] Rana Malek,[1] Weiping Chen,[4] Patricia Zerfas,[5] Duan Zhigang,[6] Elizabeth C. Wright,[6] Christina Stuelten,[7] Peter Sun,[8] Scott Lonning,[9] Monica Skarulis,[1] Anne E. Sumner,[1] Toren Finkel,[2] and Sushil G. Rane[1,*]

[1]Diabetes, Endocrinology, and Obesity Branch, National Institute of Diabetes & Digestive & Kidney Diseases
[2]Center for Molecular Medicine, National Heart, Lung, and Blood Institute
[3]Mouse Metabolism Core Laboratory
[4]Genomics Core Facility
[5]Office of Research Services, Office of the Director
[6]Office of Research Services, National Institute of Diabetes & Digestive & Kidney Diseases
[7]National Cancer Institute
[8]National Institute of Allergy and Infectious Diseases
National Institutes of Health, Clinical Research Center, South Drive and Old Georgetown Road, Bethesda, MD 20892, USA
[9]Genzyme Corporation, 5 Mountain Road, Framingham, MA 01701, USA
[10]Departamento de Bioquímica, Facultad de Medicina, Universidad de la República, Montevideo, Uruguay
*Correspondence: ranes@mail.nih.gov
DOI 10.1016/j.cmet.2011.04.013

SUMMARY

Imbalances in glucose and energy homeostasis are at the core of the worldwide epidemic of obesity and diabetes. Here, we illustrate an important role of the TGF-β/Smad3 signaling pathway in regulating glucose and energy homeostasis. Smad3-deficient mice are protected from diet-induced obesity and diabetes. Interestingly, the metabolic protection is accompanied by *Smad3*$^{-/-}$ white adipose tissue acquiring the bioenergetic and gene expression profile of brown fat/skeletal muscle. *Smad3*$^{-/-}$ adipocytes demonstrate a marked increase in mitochondrial biogenesis, with a corresponding increase in basal respiration, and Smad3 acts as a repressor of PGC-1α expression. We observe significant correlation between TGF-β1 levels and adiposity in rodents and humans. Further, systemic blockade of TGF-β signaling protects mice from obesity, diabetes, and hepatic steatosis. Together, these results demonstrate that TGF-β signaling regulates glucose tolerance and energy homeostasis and suggest that modulation of TGF-β activity might be an effective treatment strategy for obesity and diabetes.

INTRODUCTION

Positive energy balance ensues when energy intake exceeds energy expenditure, leading to net storage of excess calories in the form of fat in the adipose tissue. Mammalian adipose tissue is broadly classified as either white adipose tissue (WAT) or brown adipose tissue (BAT). WAT functions as an energy storage depot characterized by large lipid droplets and is a prominent endocrine organ, producing hormones that regulate feeding and satiety (Rosen and Spiegelman, 2006). In contrast, BAT is an energy dissipation depot characterized by densely packed mitochondria and unique expression of uncoupling protein-1 (UCP1) (Cannon and Nedergaard, 2004, 2011). Interestingly, three distinct tissues—the dermis, muscle, and brown fat—originate from the central dermomyotome (Atit et al., 2006). Immature undifferentiated brown fat cells harbor muscle-specific transcripts, and microarray analyses revealed that brown preadipocytes exhibit a myogenic transcriptional signature (Timmons et al., 2007). Intrascapular BAT appears developmentally related to skeletal muscle, with both tissues harboring abundant mitochondria, and the transcription factor PRDM16 determines the fate of precursor cells toward brown fat cells (Seale et al., 2008, 2009). Recent findings that metabolically active BAT stores exist in humans (Nedergaard et al., 2007) have stimulated interest concerning the therapeutic potential of augmenting BAT to combat metabolic diseases (Enerbäck, 2010; Nedergaard and Cannon, 2010).

Interestingly, brown adipocytes are also observed interspersed within WAT in response to cold exposure or upon stimulation by β-adrenergic pathways (Cousin et al., 1992; Guerra et al., 1998). However, intrascapular BAT and brown adipocytes interspersed within the WAT may have distinct origins, and their development may be regulated by different genetic programs (Xue et al., 2007). Accumulating evidence has prompted the classification of adipocytes into three subtypes: the brown adipocyte, the white adipocyte, and the brown adipocytes in WAT (Petrovic et al., 2010). Identification of signaling pathways that regulate acquisition of BAT properties by WAT could foster development of novel therapies for obesity and T2D.

TGF-β and its related factors control the development, growth, and function of diverse cell types (Shi and Massagué, 2003). TGF-β transmits its signals via dual serine/threonine kinase receptors and transcription factors called Smads, with Smad3 serving as the principal facilitator of TGF-β signals (Feng and Derynck, 2005). TGF-β levels correlate with obesity in mice (Samad et al., 1997, 1999) and humans (Alessi et al., 2000;

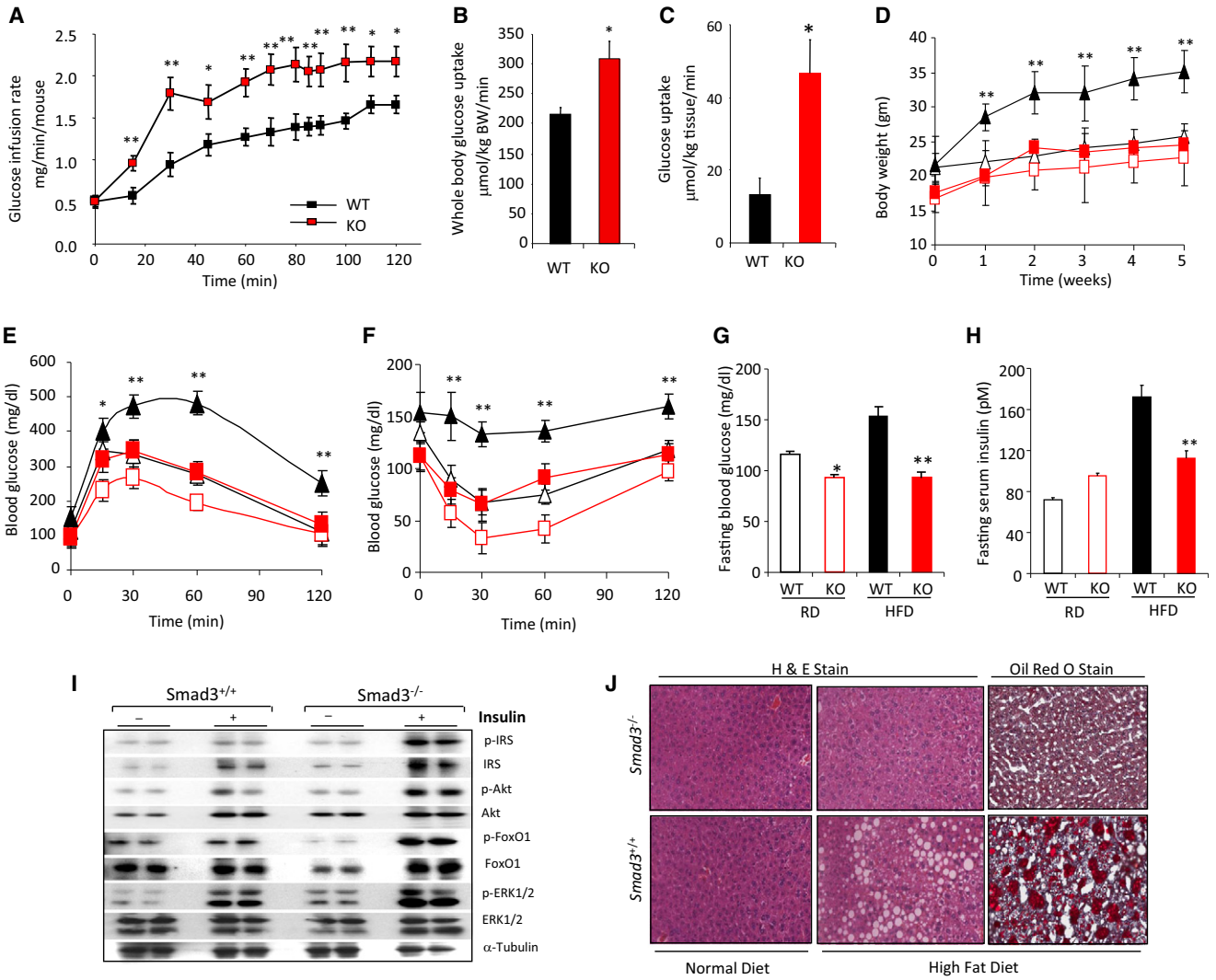

Figure 1. Smad3 Loss Protects against Diet-Induced Obesity, Insulin Resistance, and Hepatic Steatosis

(A–C) Increased glucose infusion rate (A), whole-body glucose uptake (B), and WAT glucose uptake (C) in *Smad3*$^{-/-}$ mice (KO), compared with *Smad3*$^{+/+}$ mice (WT).

(D–F) Lower-body weight gain (D), improved glucose (E) and insulin (F) tolerance in KO mice fed either a regular diet (RD; open red symbols) or high-fat diet (HFD; closed red symbols) compared to WT mice fed a RD (open black symbols) or HFD (closed black symbols).

(G and H) HFD-fed KO mice showed significantly lower glucose (G) and insulin (H) levels compared to WT mice fed a HFD.

(I) Enhanced insulin receptor signaling activity in *Smad3*$^{-/-}$ WAT.

(J) HFD-fed *Smad3*$^{-/-}$ mice, but not HFD-fed *Smad3*$^{+/+}$ mice, are resistant to hepatic steatosis. *$p < 0.05$; **$p < 0.005$; ***$p < 0.001$.

Fain et al., 2005; Lin et al., 2009b). We recently described an important role of the TGF-β/Smad3 pathway in regulation of insulin gene transcription and β cell function (Lin et al., 2009a). However, the importance of TGF-β signaling in energy homeostasis and pathogenesis of diabetes and obesity is largely obscure and a focus of this study.

RESULTS

Smad3 Loss Protects against Diet-Induced Obesity and Insulin Resistance

During a hyperinsulinemic-euglycemic clamp experiment, *Smad3*$^{-/-}$ mice exhibit enhanced insulin sensitivity, as evidenced by elevated glucose infusion rate (Figure 1A) and increased whole-body glucose uptake (Figure 1B). Increased glucose uptake was particularly marked in WAT (Figure 1C) as opposed to other metabolically active tissues, such as skeletal muscle (data not shown). When challenged with high-fat diet (HFD), *Smad3*$^{-/-}$ mice gained less weight (Figure 1D) and exhibited enhanced glucose tolerance (Figure 1E) and insulin sensitivity (Figure 1F), leading to lower fasting blood glucose and insulin levels (Figures 1G and 1H). Further, we observed increased activation of the insulin receptor signaling pathway in *Smad3*$^{-/-}$ WAT (Figure 1I). HFD-fed *Smad3*$^{+/+}$ mice developed hepatic steatosis, a condition frequently observed during insulin resistance, characterized by ectopic fat deposition in liver

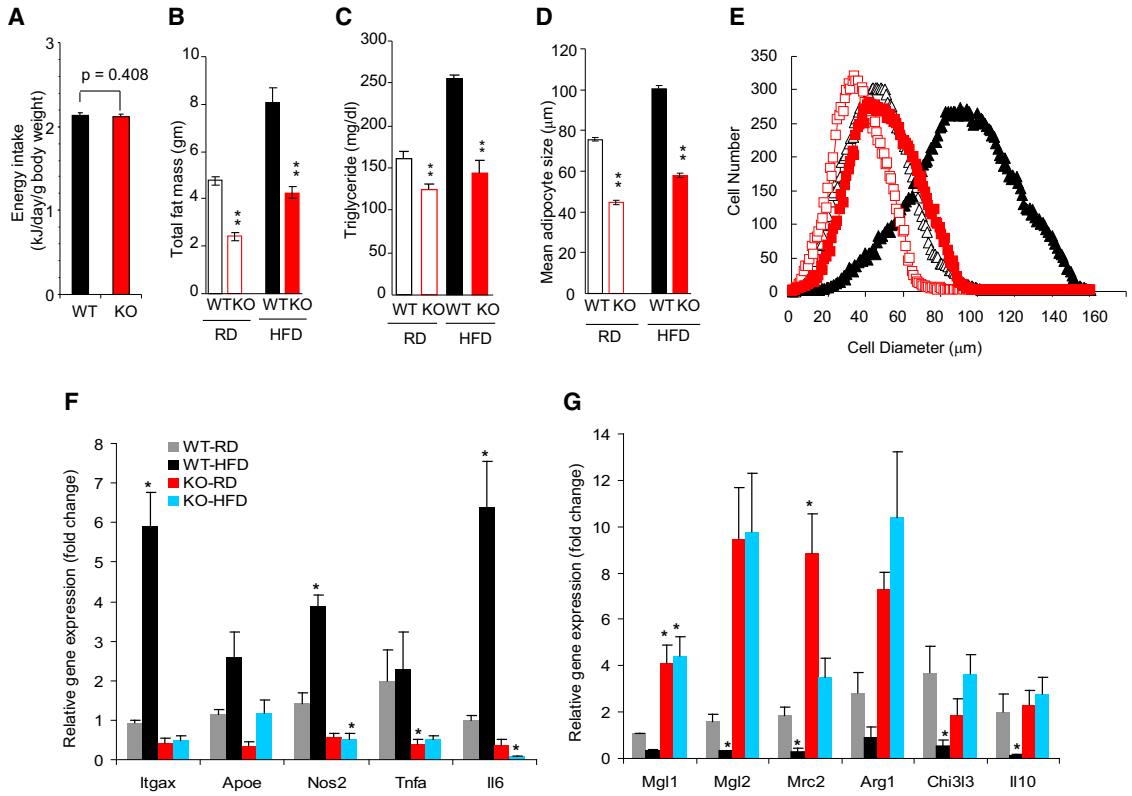

Figure 2. Smad3 Deficiency Suppresses White Adipose Tissue Differentiation

(A) WT and KO mice intake similar caloric energy, as monitored by weekly food intake.

(B and C) RD-fed or HFD-fed KO mice harbor reduced fat mass (B) and triglyceride levels (C).

(D and E) KO adipocytes (red) on a RD (open symbols) or HFD (closed symbols) maintain smaller size compared to WT adipocytes (black).

(F and G) KO mice fed RD or HFD exhibit significantly reduced levels of inflammatory M1 macrophage-specific transcripts (F) and increased levels of protective M2 macrophage-specific transcripts (G). *p < 0.05; **p < 0.005; ***p < 0.001.

tissue (Figure 1J). Remarkably, HFD-fed *Smad3*$^{-/-}$ mice were protected from hepatic steatosis (Figure 1J). These results illustrate that Smad3 deficiency confers enhanced insulin sensitivity and prevents HFD-induced obesity, insulin resistance, and hepatic steatosis.

Smad3 Loss Induces WAT to BAT Phenotypic Transition

The observed differences in body weight between wild-type and *Smad3*$^{-/-}$ mice were not due to differences in caloric intake (Figure 2A). Interestingly, *Smad3*$^{-/-}$ mice display significantly reduced fat mass (Figure 2B), which, taken together with the enhanced glucose uptake in the WAT (Figure 1C), prompted examination of the WAT compartment in greater detail. *Smad3*$^{-/-}$ MEFs were markedly impaired in their ability to differentiate into white adipocytes (Figure S1A). Consistent with these results, we also observed reduced expression of white adipocyte-specific genes in *Smad3*$^{-/-}$ MEFs (data not shown) and in *Smad3*$^{-/-}$ WAT (Figure S1B). Furthermore, WAT-derived (Figure S1D) and circulating levels of triglyceride (Figure 2C), leptin, and resistin (Figures S1E and S1F) were significantly reduced in *Smad3*$^{-/-}$ mice. Immunofluorescence staining for the WAT-specific protein, perilipin, revealed reduced adipocyte size in *Smad3*$^{-/-}$ WAT (Figures 2D, 2E, and S1C). *Smad3*$^{-/-}$ mice also exhibited reduced levels of inflammatory cytokines and less inflammatory macrophage infiltration into WAT, with a switch in macrophage spectrum from inflammatory M1 to protective M2 macrophages (Lumeng et al., 2007) (Figures 2F, 2G, and S1G–S1J).

The observed reduction in fat mass (Figure 2B) and the overall smaller adipocyte size (Figures 2D and 2E) led us to postulate that *Smad3*$^{-/-}$ WAT may harbor features that promote energy dissipation. As expected, *Smad3*$^{+/+}$ WAT appeared pale white in color and comprised predominantly large unilocular adipocytes (Figure 3A). In contrast, *Smad3*$^{-/-}$ WAT possessed a dark-red color and was comprised of smaller and multilocular adipocytes interspersed within the milieu of larger unilocular white adipocytes (Figure 3A)—a morphology that resembled brown adipocytes (Cousin et al., 1992). Consistent with this notion, we observed that many cells in the *Smad3*$^{-/-}$ WAT stained positive for UCP1 (Figure 3B), a marker uniquely present in brown adipocytes. In contrast, UCP1^{+} cells were absent in *Smad3*$^{+/+}$ WAT. Further, we observed increased mRNA expression of markers of brown adipogenesis (Seale et al., 2009), i.e., PGC-1α, UCP1, and PRDM16 in *Smad3*$^{-/-}$ WAT (Figure 3C), and UCP1 protein level was also increased (Figure 3D). To further characterize the role of Smad3, we established a 3T3-L1 preadipocyte cell-based system where Smad3 expression was knocked down using a lentivirus expressing short hairpin RNA

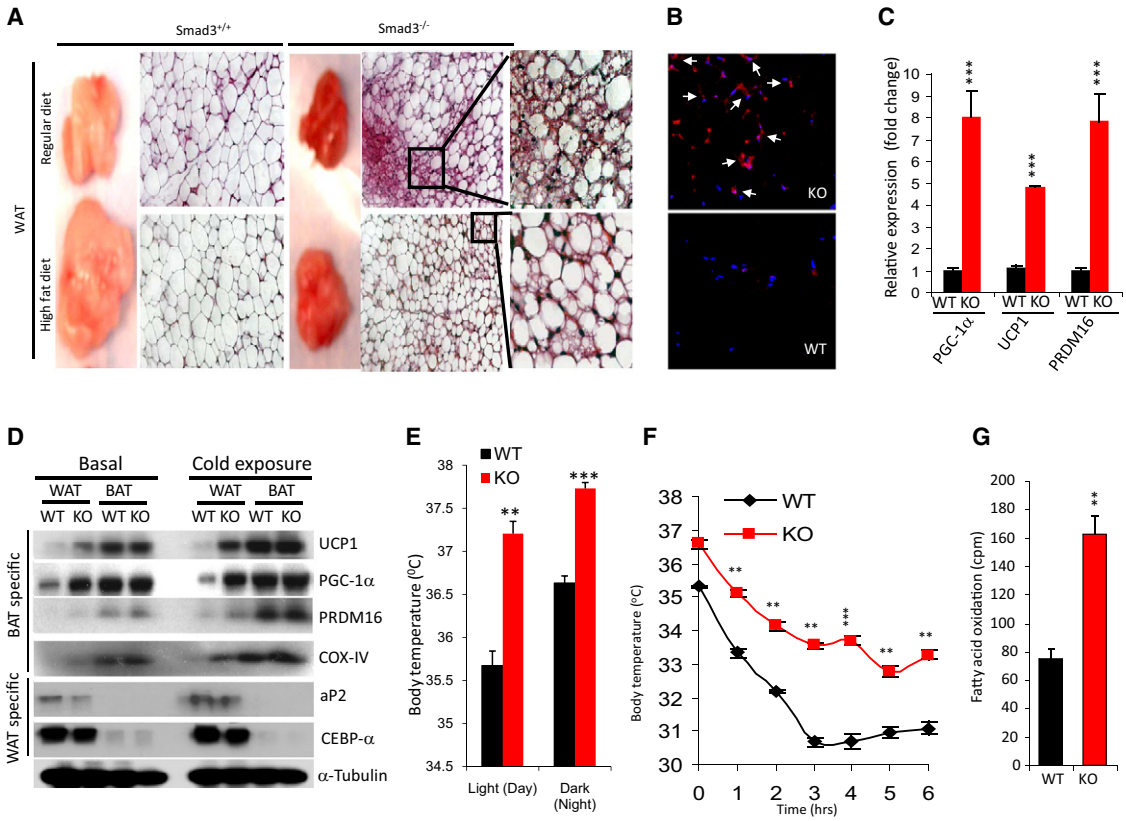

Figure 3. Smad3 Loss Induces White Fat to Brown Fat Phenotypic Transition

(A) RD-fed or HFD-fed *Smad3*$^{-/-}$ mice harbor reduced fat mass and smaller adipocytes.

(B) UCP1 expression in KO WAT (arrows).

(C) KO WAT displays enhanced expression of BAT-specific genes.

(D) KO WAT displays increased expression of BAT/mitochondrial-specific proteins and reduced expression of WAT-specific proteins.

(E and F) KO mice exhibit significant elevation in body temperature during day and night (active) conditions (E) and defend against extended cold exposure (F).

(G) KO mice exhibit enhanced fatty acid oxidation in their primary adipocytes. *p < 0.05; **p < 0.005; ***p < 0.001.

against Smad3 (shSmad3). Upon treatment with white adipocyte differentiation medium, 3T3-L1 cells expressing shSmad3 showed elevated mRNA and protein expression of BAT-specific markers (PGC-1α, UCP1, Cidea), as compared to 3T3-L1 cells infected with a control lentivirus (Figures S2A and S2B). Together, these results emphasize that loss of Smad3 signal promotes acquisition of brown adipocyte features in white adipocytes.

UCP1 and PGC-1α typically are activated in the BAT upon cold exposure (Cannon and Nedergaard, 2004). To compare the relative expression of these genes in WAT and BAT, we performed real-time RT-PCR analyses using basal and cold-activated BAT and WAT tissue from *Smad3*$^{-/-}$ and *Smad3*$^{+/+}$ mice. We observed significantly elevated gene expression of BAT-specific genes in *Smad3*$^{-/-}$ epididymal WAT, both in basal and cold-exposure conditions (Table S1). Moreover, protein levels of BAT-specific markers were significantly increased in *Smad3*$^{-/-}$ WAT (Figure 3D). As expected, the degree of expression of BAT-specific markers was higher in the intrascapular BAT compared to that observed in WAT (Figure 3D). Taken together, these observations are consistent with an active brown adipogenesis program in *Smad3*$^{-/-}$ WAT. The protein expression of brown adipocyte markers, although higher than that seen in WAT, was similar in the *Smad3*$^{-/-}$ and *Smad3*$^{+/+}$ BAT both during basal and cold-exposure conditions (Figure 3D). However, we observed a significant increase in BAT-specific transcripts in cold-activated *Smad3*$^{-/-}$ BAT, compared to cold-activated *Smad3*$^{+/+}$ BAT (Table S1). Taken together, we suggest that Smad3 loss promotes acquisition of brown fat features in the white fat.

We next inquired whether the occurrence of brown adipocytes in the WAT was of physiological relevance. *Smad3*$^{-/-}$ mice exhibit higher basal body temperature during day and night (active) conditions (Figure 3E). Moreover, *Smad3*$^{-/-}$ mice were able to maintain significantly higher body temperature when exposed to cold for an extended time (Figure 3F). Interestingly, we also observed significantly elevated fatty acid oxidation in *Smad3*$^{-/-}$ adipocytes (Figure 3G).

Smad3 Loss Promotes Mitochondrial Biogenesis and Function in WAT

Brown adipocytes, akin to skeletal muscle cells, demonstrate abundant mitochondria. Our data demonstrate that *Smad3*$^{-/-}$ WAT exhibits increased expression of PGC-1α, the master

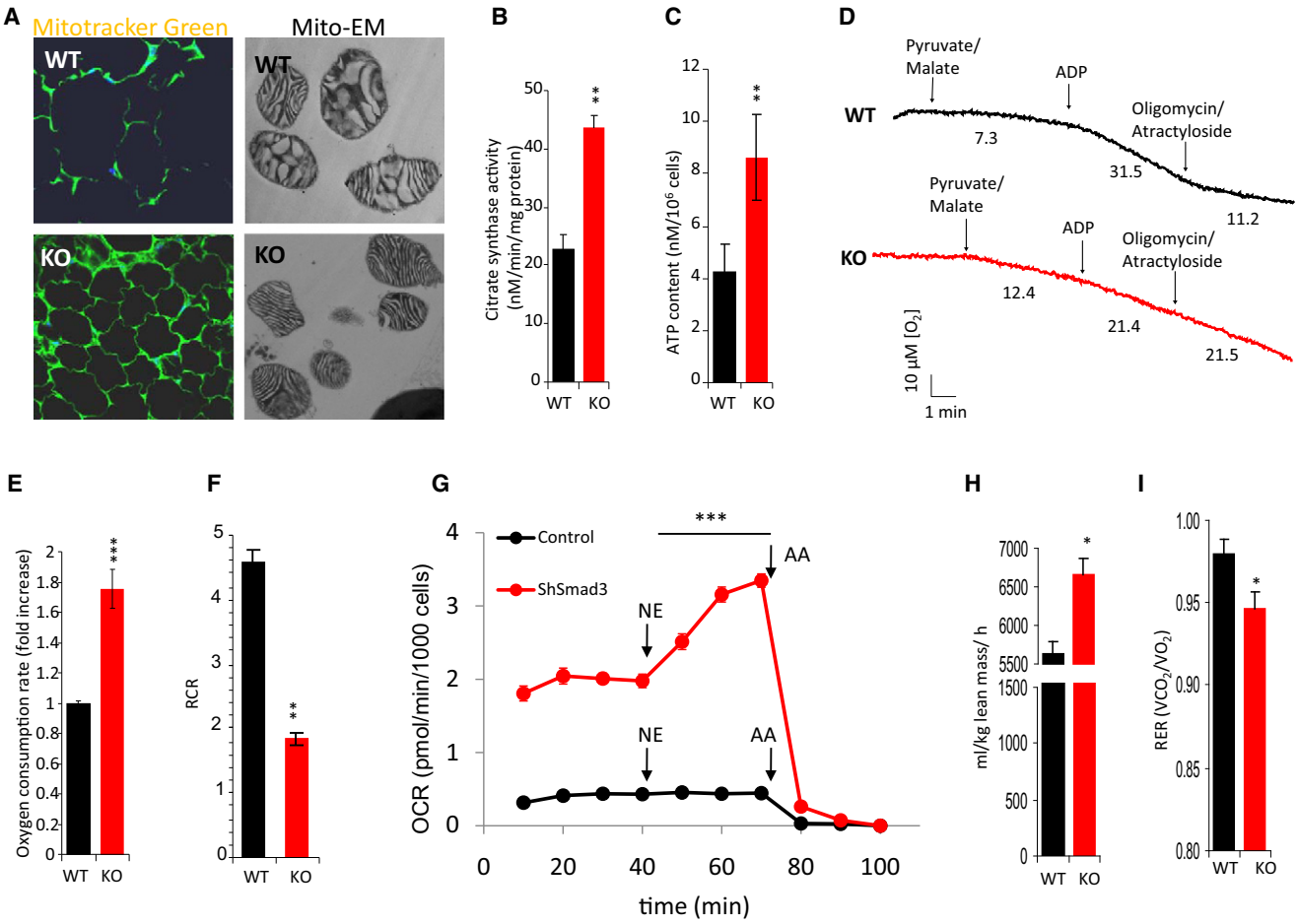

Figure 4. Smad3 Loss Promotes Mitochondrial Biogenesis and Function in WAT

(A) MitoTracker green fluorescence in adipocytes and electron microscopy in WAT mitochondria (Mito-EM).

(B and C) KO adipocytes exhibit significantly elevated citrate synthase activity (B) and ATP content (C).

(D) Representative oxygen consumption by mitochondria isolated from WAT in the presence of pyruvate/malate, ADP, and the inhibitors oligomycin and actractyloside. The oxygen consumption rate (nmol/min/mg prot) is shown below the trace after the addition of the mentioned substrates and inhibitors.

(E) KO primary adipocytes exhibit significantly increased oxygen consumption. The fold differences in oxygen consumption are derived from the calculated slope of oxygen utilization.

(F) Respiratory control ratio (RCR) (State3/State4) of isolated WAT mitochondria demonstrating increased mitochondrial uncoupling, as evidenced by a lower RCR, in KO tissue (n = 4 separate mitochondrial preparations per genotype).

(G) Oxygen consumption rate (OCR) is increased in intact shSmad3 lentivirus-infected 3T3-L1 cells in basal conditions and further enhanced by the addition of 1 μM norepinephrine (NE). NE does not affect OCR in control cells. The addition of complex III inhibitor antimycin A (AA) inhibits respiration in both cells. For basal OCR versus OCR after NE addition, control versus ShSmad3 is $p < 0.001$ for all measurements.

(H and I) Resting oxygen consumption at 20°C (H) and respiratory exchange ratio (I) in 3-month-old female *Smad3*$^{+/+}$ (WT) and *Smad3*$^{-/-}$ (KO) mice fed chow diet.

*$p < 0.05$; **$p < 0.005$; ***$p < 0.001$.

regulator of mitochondrial biogenesis. To understand the functional importance of this augmented expression, we next sought to assess mitochondrial number and activity in *Smad3*$^{-/-}$ WAT. Consistent with the observed increase in PGC-1α, *Smad3*$^{-/-}$ WAT exhibited increased staining of the mitochondria-specific fluorophore Mito-Tracker Green (Figure 4A) and increased mitochondrial DNA copy number (Figure S3A). Furthermore, morphological evaluation by electron microscopy of mitochondria derived from *Smad3*$^{-/-}$ WAT revealed organelles with densely packed cristae (Figure 4A), a feature characteristic of brown adipocyte mitochondria (Cousin et al., 1992). Further, *Smad3*$^{-/-}$ WAT exhibited elevated citrate synthase activity (Figure 4B), consistent with enhanced mitochondrial content or function. We also observed an increase in basal ATP content (Figure 4C). In addition, we observed significantly increased expression of mitochondrial-specific transcripts in *Smad3*$^{-/-}$ WAT, under basal and cold-exposure conditions (Table S1 and Figure S3D). This phenomenon appeared cell autonomous since 3T3-L1 cells expressing shSmad3 showed elevated gene expression of mitochondrial specific markers (Figure S3E). Finally, we also observed elevated protein expression of multiple essential mitochondrial gene products (Wilson-Fritch et al., 2004), ATP synthase, and cytochrome oxidase in 3T3-L1 cells expressing shSmad3 lentivirus and in *Smad3*$^{-/-}$ WAT (Figures S2B and S2C).

Evaluation of isolated mitochondria from WAT of *Smad3*$^{+/+}$ or *Smad3*$^{-/-}$ mice demonstrated that in the presence of the Complex I-dependent substrates pyruvate/malate, *Smad3*$^{-/-}$ mitochondria had increased rates of basal respiration (Figure 4D and Table S2). This observation was consistent with the observed increase in the basal rate of oxygen consumption in intact *Smad3*$^{-/-}$ primary adipocytes (Figure 4E). Although basal rates of respiration were lower in *Smad3*$^{+/+}$ mitochondria, following addition of ADP, the oxygen consumption rate (state 3 respiration) increased by approximately 4-fold (Figure 4D and Table S2). In contrast, consistent with increased uncoupling in the isolated mitochondria, less than a 2-fold increase in oxygen consumption rate was observed following ADP addition to the *Smad3*$^{-/-}$ mitochondria. Addition of oligomycin and atractyloside, agents that block proton conductance through the ATP synthase and adenine nucleotide translocator, respectively, inhibited oxygen consumption in *Smad3*$^{+/+}$ mitochondria but not in mitochondria derived from *Smad3*$^{-/-}$ mice. However, consistent with increased uncoupling of the isolated mitochondria, oligomycin-resistant respiration in WAT mitochondria from *Smad3*$^{-/-}$ mice was effectively inhibited by the addition of GDP (Shabalina et al., 2004), a known inhibitor of UCP1 (Figure S4B). These results were also supported by a marked difference in the respiratory control ratio (Figure 4F) between *Smad3*$^{+/+}$ and *Smad3*$^{-/-}$ mitochondria. Finally, in support of the notion that deletion of Smad3 results in a brown fat bioenergetic phenotype, we noted that when compared to control infected cells, 3T3 L1 cells expressing shSmad3 exhibited higher basal oxygen consumption (Figures 4G and S4A), presumably due to increased mitochondrial number. In shSmad3 cells, respiration could be further augmented by the addition of norepinephrine (Figure 4G), a potent activator of UCP1 activity in brown fat (Matthias et al., 2000). *Smad3*$^{-/-}$ mice also showed increased metabolic rate, adjusted to lean mass or to total body weight, both at 20°C and at 30°C (Figures 4H and S4D–S4F). Further, *Smad3*$^{-/-}$ mice exhibited lower respiratory exchange ratio (RER) (Figure 4I), in agreement with the observed increase in mitochondrial function and lipid oxidation (Figure 3G).

Ablation of TGF-β/Smad3 Signal Induces BAT/Skeletal Muscle Signature in WAT

To comprehensively delineate TGF-β/Smad3-regulated transcriptional targets that control acquisition of brown fat features by WAT, we performed microarray analyses of WAT isolated from *Smad3*$^{+/+}$ and *Smad3*$^{-/-}$ mice fed either RD or HFD. In addition, we performed microarray analyses of WAT from diet-induced obese (DIO) mice treated with an anti-TGF-β neutralization antibody (1D11) or with the isotype control 13C4 antibody (IgG). Interestingly, unsupervised cluster analyses showed that WAT from *Smad3*$^{-/-}$ mice and from mice treated with 1D11 exhibit highly significant increases in transcripts that correspond to BAT, mitochondrial function, and skeletal muscle biology (Figure 5A). Moreover, hierarchical clustering revealed a "signature" of 103 genes that predominantly include regulators of BAT/mitochondria (such as PGC-1α, Ucp1, Dio2, Cidea, and cytochrome *c* oxidase) and skeletal muscle biology (such as myosin, troponin, and tropomyosin) (Figure 5B and Table S3). These results demonstrate that suppression of TGF-β/Smad3 signaling promotes the acquisition of a BAT/skeletal muscle phenotype in WAT. Furthermore, we observed significantly increased expression of skeletal muscle-specific genes in basal and cold-activated *Smad3*$^{-/-}$ WAT (Table S1). Together, these observations are consistent with the link between brown fat and skeletal muscle (Seale et al., 2008).

PGC-1α is a transcriptional coactivator that regulates genes involved in energy metabolism and provides a direct link between external physiological circuits and the regulation of mitochondrial biogenesis (Lin et al., 2005). TGF-β target genes are regulated by binding of Smad3 to Smad-binding elements (SBEs) on gene promoters (Feng and Derynck, 2005), and sequence analysis revealed the presence of SBEs on the PGC-1α promoter. Chromatin immunoprecipitation (ChIP) assays showed evidence of Smad3 binding to the PGC-1α promoter in 3T3-L1 cells (Figure 5C). Furthermore, TGF-β suppressed the PGC-1α luciferase reporter in 3T3-L1 cells, whereas TGF-β was unable to repress the promoter in 3T3-L1 cells expressing shSmad3 (Figure 5D), indicating that TGF-β represses the PGC-1α promoter in a Smad3-dependent manner.

We next developed a 3T3-L1 cell-based system where, via lentivirus-based shRNA technology, we could reduce expression of Smad3 and PRDM16 either individually or in combination and analyze the resultant effects on BAT and WAT-specific gene expression. As expected, knockdown of PRDM16 repressed expression of BAT-specific genes, while the levels of WAT-specific genes were elevated (Figure 5E). In contrast, Smad3 knockdown resulted in upregulation of BAT-specific genes and repression of the WAT-specific genes (Figure 5E). Interestingly, knockdown of Smad3 and PRDM16 together yielded an intermediate phenotype wherein the effects of Smad3 in repressing BAT-specific gene expression or that of PRDM16 in promoting BAT-specific gene expression were effectively neutralized (Figure 5E). Together, these results support the notion of Smad3 regulating the appearance of brown-like adipocytes in the WAT by regulating the PGC-1α-PRDM16 axis (Figure 5F).

TGF-β1 Levels Positively Correlate with Adiposity, and Exogenous TGF-β1 Represses BAT/Mitochondrial Genes

While the findings thus far supported the concept that reduced TGF-β/Smad3 signals are beneficial to glucose and energy homeostasis, they also suggested that elevated TGF-β levels might promote glucose intolerance and obesity. We examined circulating TGF-β1 levels in a total of 184 nondiabetic human subjects of diverse ethnic origin derived from two studies: Study I exclusively included blacks of African American descent (Sumner et al., 2005), and Study 2 included subjects of diverse ethnic origin (Caucasian, Black, Hispanic, and Asian) (Table S4). Subjects had normal liver function tests and were primarily devoid of liver fibrosis and fatty liver disease. TGF-β1 levels were similar between men and women ($p = 0.079$) and between black subjects and nonblack subjects ($p = 0.75$). Circulating TGF-β1 levels were not correlated with age ($r = 0.07$, $p = 0.32$). Significant correlations between TGF-β1 levels and BMI, fat mass, and VO_2 consumption in the subjects suggested that elevated TGF-β1 levels associate with poor metabolic profile in human subjects (Table S4). After adjusting for age and fasting insulin level, the partial correlation between BMI and TGF-β1 was statistically significant (Figure 6A;

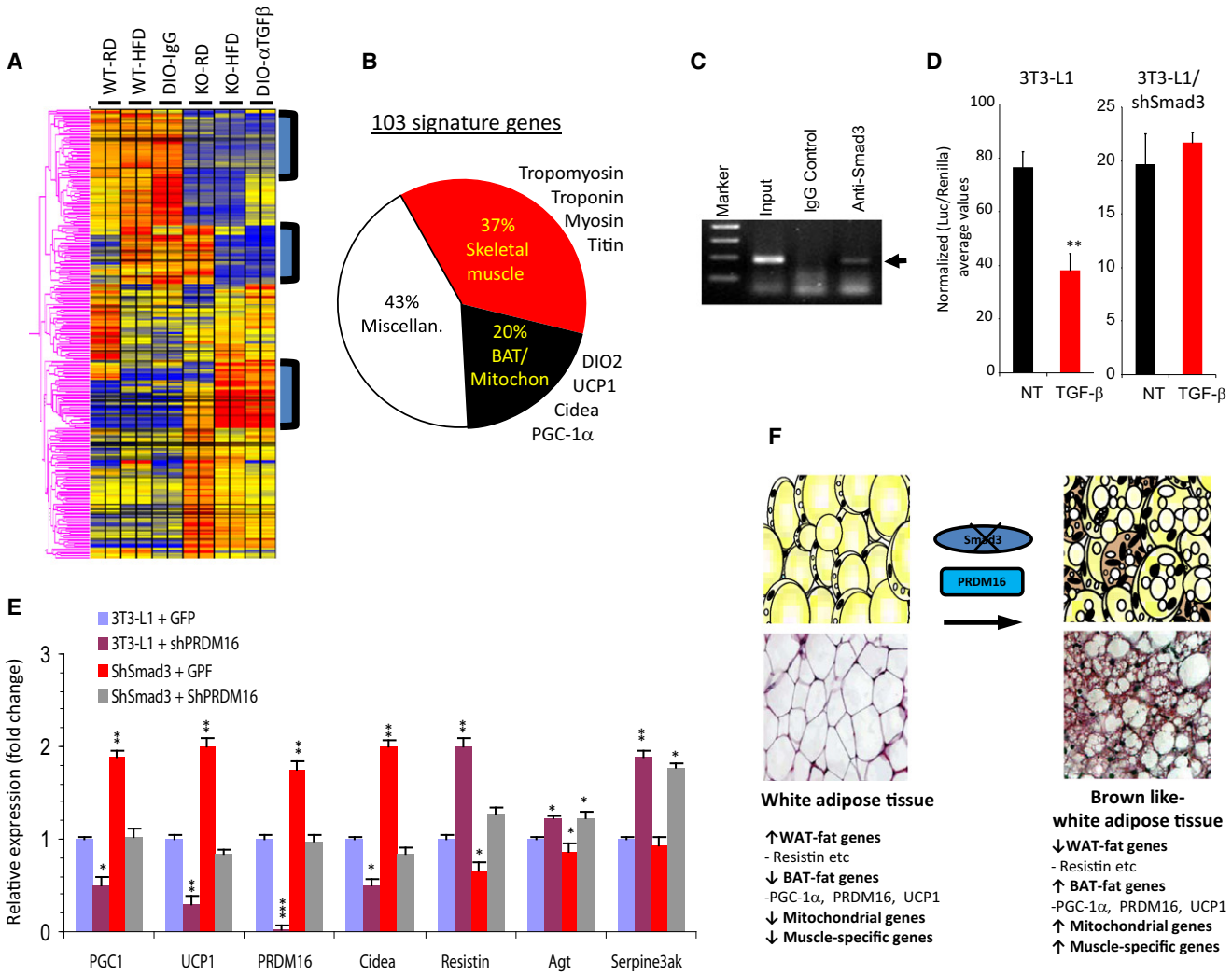

Figure 5. Smad3 Regulates the PGC-1α Promoter and PRDM16 Target Genes

(A) Representative heat map of microarray analyses of WAT from RD- or HFD-fed WT and KO mice and from diet-induced obese (DIO) mice treated with control IgG or anti-TGF-β (α-TGF-β) antibody.

(B) Pie-chart classification of "103 signature genes" (represented in the three boxed areas of the heat map) in WAT from RD- or HFD-fed KO mice and from DIO mice treated with α-TGF-β antibody, compared to RD- or HFD-fed WT mice and from DIO mice treated with control IgG, respectively.

(C) ChIP assays show binding of Smad3 (arrowhead) to the PGC-1α promoter in 3T3-L1 cells. Input and IgG antibody control is shown.

(D) TGF-β suppresses the PGC-1α-luciferase reporter in 3T3-L1 cells, but not in 3T3-L1 cells expressing shSmad3 lentivirus.

(E) Smad3 regulates PRDM16 target genes. Control 3T3-L1 cells were infected with lentiviruses expressing GFP (3T3-L1GFP), shPRDM16 (3T3-L1 + shPRDM16), shSmad3 (shSmad3 + GFP), or shSmad3 and ShPRDM16 together (shSmad3 + shPRDM16), followed by real-time RT-PCR. Fold change in expression relative to 18S is shown.

(F) Proposed model for WAT to BAT phenotypic conversion upon loss of Smad3 signaling. Loss of Smad3 leads to enhanced expression of BAT/mitochondrial/muscle-specific transcripts along with reduced expression of WAT-specific genes. The appearance of UCP1$^+$ brown adipocytes in the WAT milieu is promoted by PRDM16. *p < 0.05; **p < 0.005; ***p < 0.001.

r = 0.287, p < 0.001). Moreover, as shown in Figure 6B, TGF-β1 levels proportionately increased with adiposity in overweight (BMI of 25–29.9 kg/m^2) and obese (BMI of >30 kg/m^2) subjects compared to normal subjects (BMI of <24.9 kg/m^2). In addition, we observed inverse correlation of TGF-β1 levels with VO_2 max (Figure S5A; r = −231, p = 0.009). Together, these results show a significant positive association between TGF-β1 and human adiposity. In addition, positive correlations were observed with fat mass, fasting insulin levels, and HOMA insulin resistance index, but not with blood pressure (DBP) and levels of fasting glucose, triglyceride, free fatty acids, and insulin sensitivity (SI) (Figures S5B–S5I).

We next examined TGF-β1 levels in Lep$^{ob/ob}$ and DIO mouse models as a function of their adiposity and diabetes. Circulating TGF-β1 levels were measured in Lep$^{ob/ob}$ mice starting at 4 weeks age (body weight 25 ± 1.3 g) until the mice doubled their body weight (53 ± 3.2 g) and exhibited insulin resistance and diabetes. Elevated TGF-β1 levels were observed as Lep$^{ob/ob}$ mice

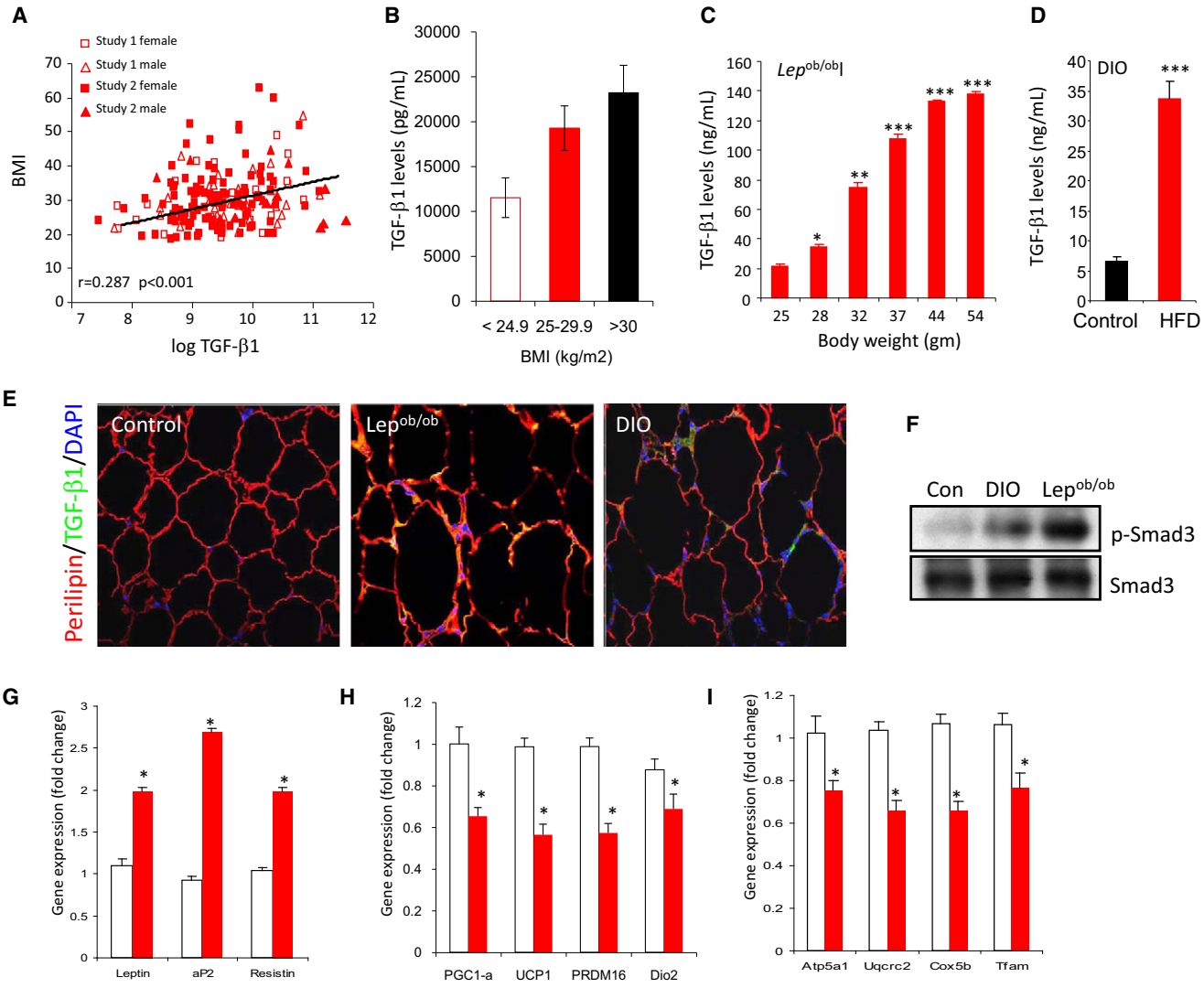

Figure 6. Elevated TGF-β1 Level Correlates with Adiposity and Exogenous TGF-β1 Suppresses BAT/Mitochondrial Markers in WAT

(A and B) Plasma TGF-β1 levels in human subjects significantly correlate positively with BM1 (A), and increased TGF-β1 levels are seen in overweight and obese subjects, compared to that seen in subjects with normal BMI (B).

(C and D) Levels of active TGF-β1 were determined by ELISA in serum samples from Lep$^{ob/ob}$ mice as a function of their weight gain (C) and in C57BL/6J mice fed either a RD (control) or HFD for 8 weeks (D).

(E) Elevated active TGF-β1 (green) staining in perilipin (red) expressing white adipocytes in WAT from Lep$^{ob/ob}$ and DIO mice, but not in WAT derived from regular diet-fed normal mice (Control). DAPI staining identifies nuclei.

(F) Elevated phosphorylated Smad3 in WAT protein extracts from Lep$^{ob/ob}$ (n = 4) and DIO (n = 4) mice, but not in WAT derived from regular diet-fed normal mice (Con; n = 3). Total Smad3 levels are shown in the bottom panel.

(G–I) Compared to vehicle PBS-injected mice (open bars), mice injected with TGF-β1 (closed red bars) exhibit elevated WAT-specific transcripts (G) and reduced BAT-specific (H) and mitochondrial-specific transcripts (I). *p < 0.05; **p < 0.005; ***p < 0.001.

gained body weight, and a significant 7-fold increase in TGF-β1 levels occurred with a doubling of the body weight of these mice (Figure 6C). TGF-β1 levels were also measured in normal wild-type mice fed a regular diet (RD) or HFD for 10 weeks. Increased body weight and insulin resistance in the HFD-fed mice was accompanied by a significant 5- to 7-fold increase in TGF-β1 levels compared to mice fed a RD for 10 weeks (Figure 6D). Moreover, elevated active TGF-β1 immunoreactivity was seen in perilipin-positive adipocytes in the WAT from Lep$^{ob/ob}$ and DIO mice (Figure 6E). Also, we observed increased levels of phosphorylated Smad3 in WAT from Lep$^{ob/ob}$ and DIO mice (Figure 6F). Interestingly, intraperitoneal injection of TGF-β1 in normal mice resulted in elevated WAT-specific transcripts (Figure 6G), whereas the expression of BAT/mitochondrial transcripts was significantly suppressed (Figures 6H and 6I).

Anti-TGF-β Antibody Protects Lep$^{ob/ob}$ and DIO Mice from Obesity and Diabetes

The studies thus far indicated a beneficial effect of suppressing TGF-β/Smad3 signals on glucose tolerance, body weight gain,

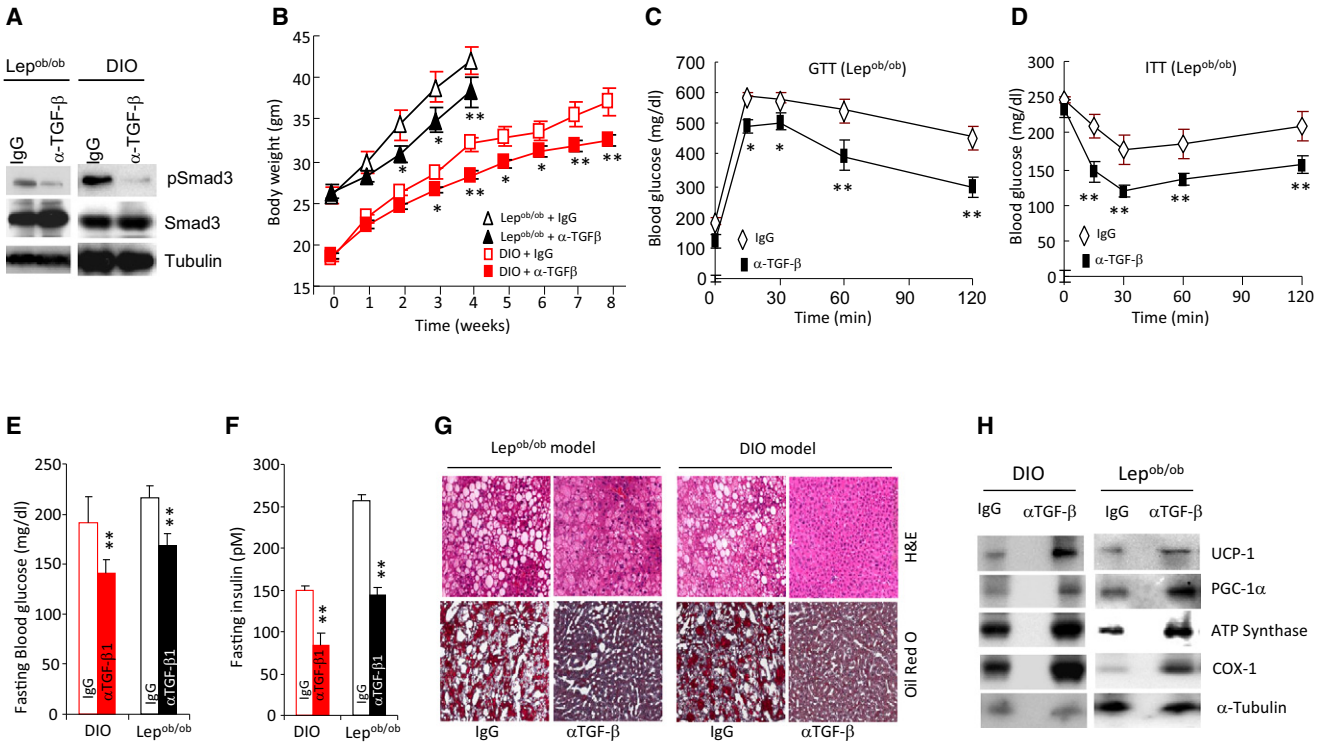

Figure 7. Anti-TGF-β Antibody Protects Lep$^{ob/ob}$ and DIO Mice from Obesity and Diabetes

(A) Reduced phosphorylated Smad3 in WAT protein extracts from Lep$^{ob/ob}$ (n = 3) and DIO (n = 3) mice treated with anti-TGF-β (α-TGF-β) antibody.

(B–H) Treatment with anti-TGF-β (α-TGF-β) antibody resulted in significantly reduced body weight gain, improved GTT (C), enhanced ITT (D), significantly reduced fasting blood glucose (E) and fasting insulin levels (F), suppression of hepatic steatosis (G), and elevated expression of BAT/mitochondrial-specific proteins in WAT (H). *p < 0.05; **p < 0.005; ***p < 0.001.

and energy homeostasis. To examine the therapeutic relevance of these findings, we evaluated the effects of the anti-TGF-β neutralization antibody (1D11) in two well-characterized mouse models of obesity and T2D. The efficacy of 1D11 (α-TGF-β) has been tested in preclinical disease models (Ling et al., 2003; Nam et al., 2008), and a closely related human version of this antibody, designated Fresolimumab, is currently being tested in human clinical studies of pulmonary fibrosis, renal disease, and cancer. We evaluated the effects of 1D11 in (1) Lep$^{ob/ob}$ mice that develop obesity and insulin resistance due to deficient leptin signaling and (2) a DIO model. As expected, antibody treatment resulted in reduction in levels of phosphorylated Smad3 in the WAT of Lep$^{ob/ob}$ and DIO mice (Figure 7A). Compared to animals treated with the isotype control 13C4 antibody (IgG), administration of 1D11 antibody suppressed body weight gain (Figure 7B), size of fat depots and fat mass (Figure S6A), adipocyte cell size (data not shown), and levels of triglyceride (Figure S6B), resistin, and leptin (data not shown). Moreover, we observed significantly reduced inflammatory F4/80+ cells (Figure S6C) and inflammatory cytokine levels, accompanied by a switch in the M1 to M2 macrophage spectrum in the WAT of antibody-treated mice (data not shown). Also consistent with the data on *Smad3*$^{-/-}$ mice, WAT from mice treated with 1D11 showed significant increases in mitochondrial DNA copy number (Figures S3B and S3C) and in transcripts that regulate BAT, mitochondrial function, and skeletal muscle biology (Figures 5A, 5B, S6E, and S6F and Table S3). Importantly, treatment with 1D11 improved glucose and insulin tolerance (Figures 7C, 7D, and S6D), suppressed hyperglycemia and hyperinsulinemia (Figures 7E and 7F), ameliorated hepatic steatosis (Figure 7G), and increased protein levels of BAT/mitochondrial markers in the WAT (Figure 7H).

DISCUSSION

Food intake in excess of metabolic needs results in continued energy storage, thereby promoting obesity and diabetes. Discovering approaches to either prevent fat storage or promote fat dissipation could have a major clinical impact. A potentially powerful approach to burn excess fat is to activate a program of thermogenesis by tissues such as the skeletal muscle and BAT that contain abundant mitochondria. Brown fat and skeletal muscle share developmental origins (Seale et al., 2008), and metabolically active BAT stores exist in humans (Nedergaard et al., 2007), opening new therapeutic avenues for obesity and diabetes (Enerbäck, 2010; Nedergaard and Cannon, 2010). There are a preponderance of data supporting the existence of brown adipocytes within the WAT milieu, although the signaling pathways that regulate the appearance of these brown adipocytes is largely obscure. Our data suggest that the TGF-β/Smad3 pathway is an important determinant of this phenomenon. In particular, we show that suppression of

TGF-β/Smad3 signaling promotes increased glucose and insulin tolerance and an overall enhanced metabolic profile. The overall effects of Smad3 deletion reported here may not be singularly attributed to changes observed in the WAT, and it is plausible that the contribution of other organs may influence the overall phenotype. Additionally, we have previously showed that Smad3 deletion results in an improved pancreatic islet β cell function (Lin et al., 2009a). We do not detect increased glucose uptake in gastrocnemius muscle, which has a high percentage of white glycolytic fibers, although glucose uptake was not normalized for fiber type. Also, we did not evaluate muscle mitochondrial measures such as mtDNA or citrate synthase activity as such studies, although important, are out of the scope of this manuscript.

The majority of the studies described here were performed using the Smad3-deficient mice maintained on a mixed 129Sv/C57BL/6 genetic background that have a variable susceptibility to a mild immune dysfunction (Yang et al., 1999). To investigate if genetic background influences the phenotypes described here, we backcrossed the 129Sv/C57BL/6-Smad3 mutant mice (Datto et al., 1999) for ten generations into a pure Balb/C genetic background. Similar to what was observed in 129Sv/C57BL/6-*Smad3*$^{-/-}$ mice, Balb/C-*Smad3*$^{-/-}$ mice exhibited reduced fat mass, lower fasting- and fed-glucose levels, improved glucose and insulin tolerance (Figures S7A–S7F), alterations in thermoregulation (Figures S7G and S7H), and elevated transcript and protein levels of BAT/mitochondrial markers (Figure S7I and Table S5).

As expected, the degree of BAT-specific marker expression is comparatively higher in BAT versus that seen in WAT. However, we find that loss of Smad3 does not lead to increased intrascapular BAT functionality per se under basal conditions or in response to cold exposure. Consistent with this, *Smad3*$^{-/-}$ MEFs differentiate toward the brown adipocytic lineage in a manner equivalent to that observed in *Smad3*$^{+/+}$ MEFs, and macro and microscopic BAT is similar in morphological appearance to that observed in *Smad3*$^{+/+}$ mice (data not shown). However, we cannot eliminate the possibility that intrascapular BAT functionality contributes to the overall metabolic phenotype. Further, the protective effects of Smad3 deletion or anti-TGF-β antibody treatment could be due to a change in the infiltrating macrophage spectrum, although it is unclear whether this is a cause or a consequence of the adiposity. Increased metabolism could also be due to an insulation phenotype, as seen in the *SCD1*$^{-/-}$ mouse (Cannon and Nedergaard, 2011; Sampath et al., 2009). However, levels of UCP1 under basal conditions are similar in BAT from *Smad3*$^{+/+}$ and *Smad3*$^{-/-}$ mice. Further, the fur in *Smad3*$^{-/-}$ mice appears normal and, in contrast to *SCD1*$^{-/-}$ mice, the *Smad3*$^{-/-}$ mice do not display cold intolerance. Thus, we infer that *Smad3*$^{-/-}$ mice do not exhibit an insulation phenomenon.

Smad3$^{-/-}$ mice were able to maintain significantly higher body temperature, even when exposed to cold for an extended time. Since the *Smad3*$^{-/-}$ mice are global knockouts, there could be a major effect on body temperature "set-point" in the hypothalamus. Technical limitations preclude us from performing simultaneous and continuous body temperature and metabolic rate measurement studies on mice administered anti-TGF-β antibody treatment. Thus, we are unable to dissociate the central and peripheral actions of TGF-β/Smad3 signals on metabolic parameters. It is plausible that the overall phenotype we describe here represents a complex phenomenon, where the absence of Smad3 has an independent central effect on body temperature with the associated metabolic increases and further has distinct effects peripherally on the phenotype of the cells developing in the WAT. Further, there may also be an increased sympathetic drive to defend the increased body temperature, which could contribute by activating the brown (and brown-like) adipocytes. We plan to dissociate the central versus peripheral actions of TGF-β/Smad3 using conditional tissue-specific knockout mice.

We suggest that the leanness and beneficial glucose homeostasis are due, at least in part, to the elevated energy expenditure as a consequence of an increased mitochondrial activity in the WAT. Increased mitochondrial uncoupling can result in a beneficial metabolic phenotype, and mouse models demonstrating increased UCP1 expression in WAT are resistant to diet-induced obesity (Narvaez et al., 2009; Polak et al., 2008). Given the increase in ATP levels (Figure 4C), we infer that the basis for increased basal oxygen consumption upon Smad3 deletion is most likely due to the increased number of mitochondria and that uncoupling is not likely to play a major role in the basal unstimulated state. Nonetheless, our data demonstrating that in shSmad3 expressing cells, adrenergic stimulation can augment respiration (Figure 4G) suggest the existence of an inducible uncoupling machinery. We suggest that the ability of TGF-β/Smad3 to modulate the overall lean phenotype is mediated by Smad3-regulating PGC-1α, which in turn controls the induction of mitochondrial biogenesis and UCP1 gene expression. Reactive oxygen species (ROS) are implicated in insulin resistance, and under certain experimental paradigms, we could detect differences in the level of ROS produced from WAT mitochondria isolated from *Smad3*$^{+/+}$ and *Smad3*$^{-/-}$ mice (Figure S4C). The precise meaning of these differences will require further experimentation.

Treatment of WAT with the PPARγ agonist rosiglitazone promotes norepinephrine-augmentable UCP1 gene expression in a subset of white adipocyte cells (Petrovic et al., 2010). Although these cells exhibit thermogenic capacity, unlike the cells we describe here, they do not express BAT/muscle-specific markers. Strikingly, global microarray analyses of the WAT, from *Smad3*$^{-/-}$ mice and mice treated with 1D11 antibody, show evidence of a unique signature of 103 genes, the majority (~60%) of which are involved in BAT, mitochondrial biology, and skeletal muscle development and function, a finding that is consistent with the nexus between brown fat and skeletal muscle (Seale et al., 2008). It is possible that a small pool of brown adipocyte precursors or a shared WAT/BAT/skeletal muscle progenitor may reside in the white fat environment. Thus, it is plausible that the TGF-β1 effect could be at the level of the common progenitor for white, brown, and muscle cells, and we are examining this possibility. Interestingly, TGF-β family members regulate differentiation either into adipocytes or myocytes in left atrium-derived pluripotent cells (Kawaguchi et al., 2010), thus further supporting the possibility of TGF-β's role in modulating the adipocyte and BAT/muscle phenotypic switch. Further, the TGF-β superfamily member, BMP7, is also implicated in brown adipogenesis (Tseng et al., 2008). We observed similar phosphorylation levels of the BMP-specific

Smad1/5/8 in *Smad3*$^{+/+}$ and *Smad3*$^{-/-}$ WAT, and stimulation of 3T3-L1 cells with BMP7 did not alter Smad3 phosphorylation (data not shown). Furthermore, the expression level of myostatin (McPherron and Lee, 2002), the TGF-β superfamily member implicated in muscle development and insulin sensitivity, and its target gene dDahl was similar in *Smad3*$^{+/+}$ and *Smad3*$^{-/-}$ WAT (data not shown). These results do not suggest a major role for BMP7 or myostatin in the observed Smad3-regulated WAT-to-BAT phenotype. TGF-β regulates adipocyte differentiation via a Smad3-C/EBP interaction (Choy and Derynck, 2003; Choy et al., 2000), and Schnurri-2 interacts with Smads and C/EBP during BMP2-regulated adipogenesis (Jin et al., 2006). Our observations of active TGF-β1 (colocalized with perilipin) and phosphorylated Smad3 in the WAT from DIO and Lep$^{ob/ob}$ mice suggests that TGF-β1 is produced in white adipocytes during conditions of adiposity or glucose intolerance, although this does not eliminate the stromal vascular fraction as a source of TGF-β1 (Fain et al., 2005). These studies, altogether, suggest an important role for TGF-β superfamily members in WAT and BAT biology, akin to the role of myostatin in muscle development (McPherron and Lee, 2002).

Intriguingly, the majority of TGF-β1 in the liver and heart is located in mitochondria, as determined by electron microscopy and cell fractionation studies (Heine et al., 1991). Our data are consistent with a potential role for TGF-β in mitochondrial function within the adipocyte with regard to energy homeostasis. Further, the recently described role for TGF-β in glucose-induced cell hypertrophy (Wu and Derynck, 2009) may have ramifications in conditions associated with hyperglycemia, glucose intolerance, and insulin resistance. Circulating TGF-β levels are elevated in cardiovascular disease and hypertension (Gordon and Blobe, 2008), and TGF-β1 and BMI are closely associated in human adipose tissue during morbid obesity (Alessi et al., 2000). Elevated TGF-β1 levels in humans correlate positively with increased adiposity and poor metabolic profile (Figure 6A) and inversely correlate with fitness, as evidenced by reduced oxygen consumption (VO_2 max) during maximal exercise testing (Figure S5A). Predisposition to various forms of cancer, atherosclerosis, myocardial infarction, hypertension, and stroke is correlated with the presence of TGF-β1 polymorphisms (Grainger et al., 1999). Further, polymorphisms such as the T29C polymorphism, which results in a Leu-Pro substitution at codon 10, are correlated with elevated circulating TGF-β levels. Interestingly, the T29C polymorphism is associated with increased BMI, elevated fasting insulin and glucose levels, and higher HOMA insulin resistance indices (Rosmond et al., 2003). Moreover, the *SMAD3* gene was identified in a type 2 diabetes genome-wide association study (Perry et al., 2009), which further supports the notion of TGF-β/Smad3 pathway as a potential target in diabetes and obesity. TGF-β antagonist approaches are being clinically evaluated to treat diseases such as cancer, fibrosis, scarring, and diabetic nephropathy where elevated TGF-β levels are implicated. The occurrence of elevated TGF-β1 levels in obese individuals combined with the beneficial effect of the anti-TGF-β neutralization antibody in mouse models of obesity and diabetes offer treatment alternatives for these diseases. In conclusion, these results offer insight into the role of TGF-β in adipose tissue biology, specifically with regard to activation of a brown adipocyte program within white fat, and a strong potential for translation of these observations for the treatment of obesity and diabetes.

EXPERIMENTAL PROCEDURES

Mice

The generation of *Smad3*$^{-/-}$ mice has been described previously (Datto et al., 1999; Yang et al., 1999). C57BL/6J and Lep$^{ob/ob}$ mice were intraperitoneally injected with 1.5 mg/kg body weight of control 13C4 antibody or anti-TGF-β antibody (1D11). All animal studies were approved by the NIDDK/NIH Animal Care and Use Committee.

Indirect Calorimetry

Three-month-old female mice were studied in an eight-chamber Oxymax system. Motor activity was determined by infrared beam interruption. Experiments were performed at 20°C and 30°C.

Euglycemic-Hyperinsulinemic Clamp and Body Composition Measurements

Insulin-stimulated whole-body glucose flux was estimated using a continuous infusion of high-pressure liquid chromatography-purified [3-^{3}H]glucose (0.1 μCi/min). Blood samples were taken for determination of plasma [^{3}H]glucose, 2-deoxy-D-[1-^{14}C]glucose, and ^3H_2O concentrations. WAT glucose uptake was calculated from the plasma 2-deoxy-D-[1-^{14}C]glucose concentration. Body composition was measured in nonanesthetized mice using Echo 3-in-1 NMR analyzer.

Glucose and Insulin Tolerance Tests

For glucose tolerance tests, overnight-fasted mice were given i.p. glucose (2 mg/g body weight). For insulin tolerance test, fed mice were given i.p. insulin (Humulin).

Mitochondrial Isolation and Intact Cell Metabolic Studies

Mitochondrial respiration was measured in a Model 210 fiber optic oxygen monitor. Pyruvate and malate (5 mM/2 mM) were used as substrates, and ADP (0.85 mM), oligomycin (0.125 mM), and atractyloside potassium salt (0.5 mM) were added to evaluate mitochondrial coupling. Respiratory control ratio was calculated as the ratio of oxygen consumption rate after (state 3) and before (state 4) ADP addition.

Luciferase Reporter Assay

We transfected 2 × 10^5 cells/well with 1 μg/well of PGC1-α promoter reporter, together with 0.1 μg/well of Renilla-luc plasmid, using FuGENE 6 transfection reagent. Cells were treated with TGF-β, and luciferase activity was estimated using Promega dual luciferase assay kit.

ChIP Assay

ChIP assay was performed using the ChIP-IT kit from Active Motif by following the manufacturer's instructions.

Human Study Subject Population

Study 1: The subjects were participants in the Triglyceride and Cardiovascular Risk in African Americans study. Study 2: Subjects were enrolled to phenotype varying degrees of obesity. The protocols were approved by the institutional review board of NIDDK.

Statistical Analysis

For mouse studies, data are expressed as mean ± SEM. Statistical significance between groups was determined using two-tailed Student's t test or one-way ANOVA. For human study analyses, a log transform was used for TGF-β1. The results were presented as mean ± SD or SEM. Pearson's correlation analysis was performed between TGF-β1 and other variables. A p value of <0.05 was considered statistically significant, and all tests were two sided. Statistical analyses were performed using SAS version 9.1 (SAS Institute, Cary, NC).

ACCESSION NUMBERS

Microarray analyses were performed using standard procedures. The data set has been deposited in the GEO public database (accession #GSE28598).

SUPPLEMENTAL INFORMATION

Supplemental Information includes seven figures, seven tables, Supplemental Experimental Procedures, and Supplemental References and can be found with this article online at doi:10.1016/j.cmet.2011.04.013.

ACKNOWLEDGMENTS

This work is dedicated to the memory of G.S. Rane. The authors appreciate the support of members of the Rane laboratory. The authors thank Alexandra McPherron (NIDDK) for advice. The technical support provided by George Poy, Madia Ricks, Anita Tambay, Ugochi Ukegbu, Richard Chen, Alice Franks, Janet Lee, William Jou, Tatyana Chanturiya, and Kevin Wang is greatly appreciated. This work was supported by funds from the NIH intramural program.

Received: October 4, 2010
Revised: February 16, 2011
Accepted: April 20, 2011
Published: July 5, 2011

REFERENCES

Alessi, M.C., Bastelica, D., Morange, P., Berthet, B., Leduc, I., Verdier, M., Geel, O., and Juhan-Vague, I. (2000). Plasminogen activator inhibitor 1, transforming growth factor-beta1, and BMI are closely associated in human adipose tissue during morbid obesity. Diabetes *49*, 1374–1380.

Atit, R., Sgaier, S.K., Mohamed, O.A., Taketo, M.M., Dufort, D., Joyner, A.L., Niswander, L., and Conlon, R.A. (2006). Beta-catenin activation is necessary and sufficient to specify the dorsal dermal fate in the mouse. Dev. Biol. *296*, 164–176.

Cannon, B., and Nedergaard, J. (2004). Brown adipose tissue: function and physiological significance. Physiol. Rev. *84*, 277–359.

Cannon, B., and Nedergaard, J. (2011). Nonshivering thermogenesis and its adequate measurement in metabolic studies. J. Exp. Biol. *214*, 242–253.

Choy, L., and Derynck, R. (2003). Transforming growth factor-beta inhibits adipocyte differentiation by Smad3 interacting with CCAAT/enhancer-binding protein (C/EBP) and repressing C/EBP transactivation function. J. Biol. Chem. *278*, 9609–9619.

Choy, L., Skillington, J., and Derynck, R. (2000). Roles of autocrine TGF-beta receptor and Smad signaling in adipocyte differentiation. J. Cell Biol. *149*, 667–682.

Cousin, B., Cinti, S., Morroni, M., Raimbault, S., Ricquier, D., Pénicaud, L., and Casteilla, L. (1992). Occurrence of brown adipocytes in rat white adipose tissue: molecular and morphological characterization. J. Cell Sci. *103*, 931–942.

Datto, M.B., Frederick, J.P., Pan, L., Borton, A.J., Zhuang, Y., and Wang, X.F. (1999). Targeted disruption of Smad3 reveals an essential role in transforming growth factor beta-mediated signal transduction. Mol. Cell. Biol. *19*, 2495–2504.

Enerbäck, S. (2010). Human brown adipose tissue. Cell Metab. *11*, 248–252.

Fain, J.N., Tichansky, D.S., and Madan, A.K. (2005). Transforming growth factor beta1 release by human adipose tissue is enhanced in obesity. Metabolism *54*, 1546–1551.

Feng, X.H., and Derynck, R. (2005). Specificity and versatility in tgf-beta signaling through Smads. Annu. Rev. Cell Dev. Biol. *21*, 659–693.

Gordon, K.J., and Blobe, G.C. (2008). Role of transforming growth factor-beta superfamily signaling pathways in human disease. Biochim. Biophys. Acta *1782*, 197–228.

Grainger, D.J., Heathcote, K., Chiano, M., Snieder, H., Kemp, P.R., Metcalfe, J.C., Carter, N.D., and Spector, T.D. (1999). Genetic control of the circulating concentration of transforming growth factor type beta1. Hum. Mol. Genet. *8*, 93–97.

Guerra, C., Koza, R.A., Yamashita, H., Walsh, K., and Kozak, L.P. (1998). Emergence of brown adipocytes in white fat in mice is under genetic control. Effects on body weight and adiposity. J. Clin. Invest. *102*, 412–420.

Heine, U.I., Burmester, J.K., Flanders, K.C., Danielpour, D., Munoz, E.F., Roberts, A.B., and Sporn, M.B. (1991). Localization of transforming growth factor-beta 1 in mitochondria of murine heart and liver. Cell Regul. *2*, 467–477.

Jin, W., Takagi, T., Kanesashi, S.N., Kurahashi, T., Nomura, T., Harada, J., and Ishii, S. (2006). Schnurri-2 controls BMP-dependent adipogenesis via interaction with Smad proteins. Dev. Cell *10*, 461–471.

Kawaguchi, N., Nakao, R., Yamaguchi, M., Ogawa, D., and Matsuoka, R. (2010). TGF-beta superfamily regulates a switch that mediates differentiation either into adipocytes or myocytes in left atrium derived pluripotent cells (LA-PCS). Biochem. Biophys. Res. Commun. *396*, 619–625.

Lin, J., Handschin, C., and Spiegelman, B.M. (2005). Metabolic control through the PGC-1 family of transcription coactivators. Cell Metab. *1*, 361–370.

Lin, H.M., Lee, J.H., Yadav, H., Kamaraju, A.K., Liu, E., Zhigang, D., Vieira, A., Kim, S.J., Collins, H., Matschinsky, F., et al. (2009a). Transforming growth factor-beta/Smad3 signaling regulates insulin gene transcription and pancreatic islet beta-cell function. J. Biol. Chem. *284*, 12246–12257.

Lin, Y., Nakachi, K., Ito, Y., Kikuchi, S., Tamakoshi, A., Yagyu, K., Watanabe, Y., Inaba, Y., and Kazuo Tajima; Jacc Study Group. (2009b). Variations in serum transforming growth factor-beta1 levels with gender, age and lifestyle factors of healthy Japanese adults. Dis. Markers *27*, 23–28.

Ling, H., Li, X., Jha, S., Wang, W., Karetskaya, L., Pratt, B., and Ledbetter, S. (2003). Therapeutic role of TGF-beta-neutralizing antibody in mouse cyclosporin A nephropathy: morphologic improvement associated with functional preservation. J. Am. Soc. Nephrol. *14*, 377–388.

Lumeng, C.N., Bodzin, J.L., and Saltiel, A.R. (2007). Obesity induces a phenotypic switch in adipose tissue macrophage polarization. J. Clin. Invest. *117*, 175–184.

Matthias, A., Ohlson, K.B., Fredriksson, J.M., Jacobsson, A., Nedergaard, J., and Cannon, B. (2000). Thermogenic responses in brown fat cells are fully UCP1-dependent. UCP2 or UCP3 do not substitute for UCP1 in adrenergically or fatty scid-induced thermogenesis. J. Biol. Chem. *275*, 25073–25081.

McPherron, A.C., and Lee, S.J. (2002). Suppression of body fat accumulation in myostatin-deficient mice. J. Clin. Invest. *109*, 595–601.

Nam, J.S., Terabe, M., Mamura, M., Kang, M.J., Chae, H., Stuelten, C., Kohn, E., Tang, B., Sabzevari, H., Anver, M.R., et al. (2008). An anti-transforming growth factor beta antibody suppresses metastasis via cooperative effects on multiple cell compartments. Cancer Res. *68*, 3835–3843.

Narvaez, C.J., Matthews, D., Broun, E., Chan, M., and Welsh, J. (2009). Lean phenotype and resistance to diet-induced obesity in vitamin D receptor knockout mice correlates with induction of uncoupling protein-1 in white adipose tissue. Endocrinology *150*, 651–661.

Nedergaard, J., and Cannon, B. (2010). The changed metabolic world with human brown adipose tissue: therapeutic visions. Cell Metab. *11*, 268–272.

Nedergaard, J., Bengtsson, T., and Cannon, B. (2007). Unexpected evidence for active brown adipose tissue in adult humans. Am. J. Physiol. Endocrinol. Metab. *293*, E444–E452.

Perry, J.R., McCarthy, M.I., Hattersley, A.T., Zeggini, E., Weedon, M.N., and Frayling, T.M.; Wellcome Trust Case Control Consortium. (2009). Interrogating type 2 diabetes genome-wide association data using a biological pathway-based approach. Diabetes *58*, 1463–1467.

Petrovic, N., Walden, T.B., Shabalina, I.G., Timmons, J.A., Cannon, B., and Nedergaard, J. (2010). Chronic peroxisome proliferator-activated receptor gamma (PPARgamma) activation of epididymally derived white adipocyte cultures reveals a population of thermogenically competent, UCP1-containing adipocytes molecularly distinct from classic brown adipocytes. J. Biol. Chem. *285*, 7153–7164.

Polak, P., Cybulski, N., Feige, J.N., Auwerx, J., Rüegg, M.A., and Hall, M.N. (2008). Adipose-specific knockout of raptor results in lean mice with enhanced mitochondrial respiration. Cell Metab. *8*, 399–410.

Rosen, E.D., and Spiegelman, B.M. (2006). Adipocytes as regulators of energy balance and glucose homeostasis. Nature *444*, 847–853.

Rosmond, R., Chagnon, M., Bouchard, C., and Björntorp, P. (2003). Increased abdominal obesity, insulin and glucose levels in nondiabetic subjects with a T29C polymorphism of the transforming growth factor-beta1 gene. Horm. Res. *59*, 191–194.

Samad, F., Yamamoto, K., Pandey, M., and Loskutoff, D.J. (1997). Elevated expression of transforming growth factor-beta in adipose tissue from obese mice. Mol. Med. *3*, 37–48.

Samad, F., Uysal, K.T., Wiesbrock, S.M., Pandey, M., Hotamisligil, G.S., and Loskutoff, D.J. (1999). Tumor necrosis factor alpha is a key component in the obesity-linked elevation of plasminogen activator inhibitor 1. Proc. Natl. Acad. Sci. USA *96*, 6902–6907.

Sampath, H., Flowers, M.T., Liu, X., Paton, C.M., Sullivan, R., Chu, K., Zhao, M., and Ntambi, J.M. (2009). Skin-specific deletion of stearoyl-CoA desaturase-1 alters skin lipid composition and protects mice from high fat diet-induced obesity. J. Biol. Chem. *284*, 19961–19973.

Seale, P., Bjork, B., Yang, W., Kajimura, S., Chin, S., Kuang, S., Scimè, A., Devarakonda, S., Conroe, H.M., Erdjument-Bromage, H., et al. (2008). PRDM16 controls a brown fat/skeletal muscle switch. Nature *454*, 961–967.

Seale, P., Kajimura, S., and Spiegelman, B.M. (2009). Transcriptional control of brown adipocyte development and physiological function—of mice and men. Genes Dev. *23*, 788–797.

Shabalina, I.G., Jacobsson, A., Cannon, B., and Nedergaard, J. (2004). Native UCP1 displays simple competitive kinetics between the regulators purine nucleotides and fatty acids. J. Biol. Chem. *279*, 38236–38248.

Shi, Y., and Massagué, J. (2003). Mechanisms of TGF-beta signaling from cell membrane to the nucleus. Cell *113*, 685–700.

Sumner, A.E., Finley, K.B., Genovese, D.J., Criqui, M.H., and Boston, R.C. (2005). Fasting triglyceride and the triglyceride-HDL cholesterol ratio are not markers of insulin resistance in African Americans. Arch. Intern. Med. *165*, 1395–1400.

Timmons, J.A., Wennmalm, K., Larsson, O., Walden, T.B., Lassmann, T., Petrovic, N., Hamilton, D.L., Gimeno, R.E., Wahlestedt, C., Baar, K., et al. (2007). Myogenic gene expression signature establishes that brown and white adipocytes originate from distinct cell lineages. Proc. Natl. Acad. Sci. USA *104*, 4401–4406.

Tseng, Y.H., Kokkotou, E., Schulz, T.J., Huang, T.L., Winnay, J.N., Taniguchi, C.M., Tran, T.T., Suzuki, R., Espinoza, D.O., Yamamoto, Y., et al. (2008). New role of bone morphogenetic protein 7 in brown adipogenesis and energy expenditure. Nature *454*, 1000–1004.

Wilson-Fritch, L., Nicoloro, S., Chouinard, M., Lazar, M.A., Chui, P.C., Leszyk, J., Straubhaar, J., Czech, M.P., and Corvera, S. (2004). Mitochondrial remodeling in adipose tissue associated with obesity and treatment with rosiglitazone. J. Clin. Invest. *114*, 1281–1289.

Wu, L., and Derynck, R. (2009). Essential role of TGF-beta signaling in glucose-induced cell hypertrophy. Dev. Cell *17*, 35–48.

Xue, B., Rim, J.S., Hogan, J.C., Coulter, A.A., Koza, R.A., and Kozak, L.P. (2007). Genetic variability affects the development of brown adipocytes in white fat but not in interscapular brown fat. J. Lipid Res. *48*, 41–51.

Yang, X., Letterio, J.J., Lechleider, R.J., Chen, L., Hayman, R., Gu, H., Roberts, A.B., and Deng, C. (1999). Targeted disruption of SMAD3 results in impaired mucosal immunity and diminished T cell responsiveness to TGF-beta. EMBO J. *18*, 1280–1291.